Aerosol size confines climate response to volcanic super-eruptions

Claudia Timmreck,[1] Hans-F. Graf,[2] Stephan J. Lorenz,[1] Ulrike Niemeier,[1]
Davide Zanchettin,[1] Daniela Matei,[1] Johann H. Jungclaus,[1] and Thomas J. Crowley[3]

Received 13 September 2010; revised 29 October 2010; accepted 9 November 2010; published 22 December 2010.

[1] Extremely large volcanic eruptions have been linked to global climate change, biotic turnover, and, for the Younger Toba Tuff (YTT) eruption 74,000 years ago, near-extinction of modern humans. One of the largest uncertainties of the climate effects involves evolution and growth of aerosol particles. A huge atmospheric concentration of sulfate causes higher collision rates, larger particle sizes, and rapid fall out, which in turn greatly affects radiative feedbacks. We address this key process by incorporating the effects of aerosol microphysical processes into an Earth System Model. The temperature response is shorter (9–10 years) and three times weaker (−3.5 K at maximum globally) than estimated before, although cooling could still have reached −12 K in some midlatitude continental regions after one year. The smaller response, plus its geographic patchiness, suggests that most biota may have escaped threshold extinction pressures from the eruption.
Citation: Timmreck, C., H.-F. Graf, S. J. Lorenz, U. Niemeier, D. Zanchettin, D. Matei, J. H. Jungclaus, and T. J. Crowley (2010), Aerosol size confines climate response to volcanic super-eruptions, *Geophys. Res. Lett.*, *37*, L24705, doi:10.1029/2010GL045464.

1. Introduction

[2] Volcanic eruptions sufficiently intense to inject material into the stratosphere affect climate primarily by the formation of sulfate aerosols, which reflect sunlight and cool the Earth. The largest explosive eruptions, so-called "super-eruptions", have been especially scrutinized because of their potentially severe impacts on climate and ecosystems [*Wignall*, 2005; *Whiteside et al.*, 2010]. The palaeoanthropological and archaeological communities continue debate as to whether an inferred "bottleneck" in human evolution [*Ambrose*, 1998; *Petraglia et al.*, 2007; *Balter*, 2010] may be related to the YTT eruption on the island of Sumatra, Indonesia. This most recent "super-eruption" took place ca. 74,000 years ago, discharging an estimated 7×10^{15} kg [*Rose and Chesner*, 1987; *Chesner et al*, 1991] of rhyolitic magma in a multitude of co-ignimbrite plumes [*Oppenheimer*, 2002]. Tephra produced by the eruption covered a vast area from the South China Sea to India and the east coast of Africa [*Self and Blake*, 2008].

[3] Early estimates suggested that the YTT eruption could have caused or triggered a shift to glacial conditions [*Rampino and Self*, 1992]. Two more recent simulations with coupled atmosphere ocean models [*Jones et al.*, 2005; *Robock et al.*, 2009] calculated a decade of severe cooling of up to −10 K (global mean) for a Toba simulation comparable to 100 times Pinatubo, but there was no further sustained cooling. Still, these previous results appear to be at odds with the high survival rate of mammalian mega fauna in South East Asia [*Louys*, 2007] and modern humans in India [*Petraglia et al.*, 2007].

[4] For estimating climatic consequences of large volcanic eruptions, the stratospheric sulfur (S) emission of the erupting magma is of central importance. For Toba this estimate varies by more than one order of magnitude (between about 10 and 360 times the stratospheric sulfur injection of the 1991 Pinatubo eruption, 8.5 Mt S) [*Oppenheimer*, 2002]. *Robock et al.* [2009] investigated the uncertainty in the sulfur emission for values in the range of 33 to 900 times the Pinatubo injection and obtained even for the lowest one a global maximum cooling of −8 K. Uncertainties in the sulfur emissions could therefore be one reason for the apparent mismatch between simulations and paleo evidence. Another possible reason for the weak response could be the decrease of volcanic radiative forcing due to aerosol growth effects for very large eruptions [*Pinto et al.*, 1989; *Timmreck et al.*, 2009], which has been neglected in previous studies. Already in 1989, Pinto et al. have discussed the possible important role of aerosol size in restricting the response to large eruptions, but this idea has so far not been tested in a climate model in combination with an aerosol microphysical model. Here, we take into account the formation and temporal development of the volcanic aerosol distribution in an Earth System Model (ESM) simulation of the YTT eruption in order to thoroughly examine the effects of the eruption on climate and life.

2. Experimental Setup

[5] A two-step modeling approach was applied to consider more realistic effects of aerosol growth and sedimentation in ESM simulations of volcanic super-eruptions. In a first step the formation of sulfate aerosol from an initial stratospheric injection of 850 Mt S (=100X Pinatubo) was calculated with the middle atmosphere version [*Niemeier et al.*, 2009] of the aerosol climate model ECHAM/HAM [*Stier et al.*, 2005], which includes a module of aerosol microphysics and a parameterized stratospheric chemistry module. For extremely large volcanic eruptions the availability of OH radicals for SO_2 oxidation is limited [*Bekki*, 1995]. This process is additionally parameterized in the model. This MAECHAM5/HAM model is applied in T42 horizontal resolution with 39 vertical layers reaching up to 0.01 hPa and calculates the temporal evolution of aerosol optical depth at 0.55 μm (AOD) and effective radius (R_{eff}).

[1]Max-Planck Institute for Meteorology, Hamburg, Germany.
[2]Centre Atmospheric Science, University of Cambridge, Cambridge, UK.
[3]School of GeoSciences, University of Edinburgh, Edinburgh, UK.

Copyright 2010 by the American Geophysical Union.
0094-8276/10/2010GL045464

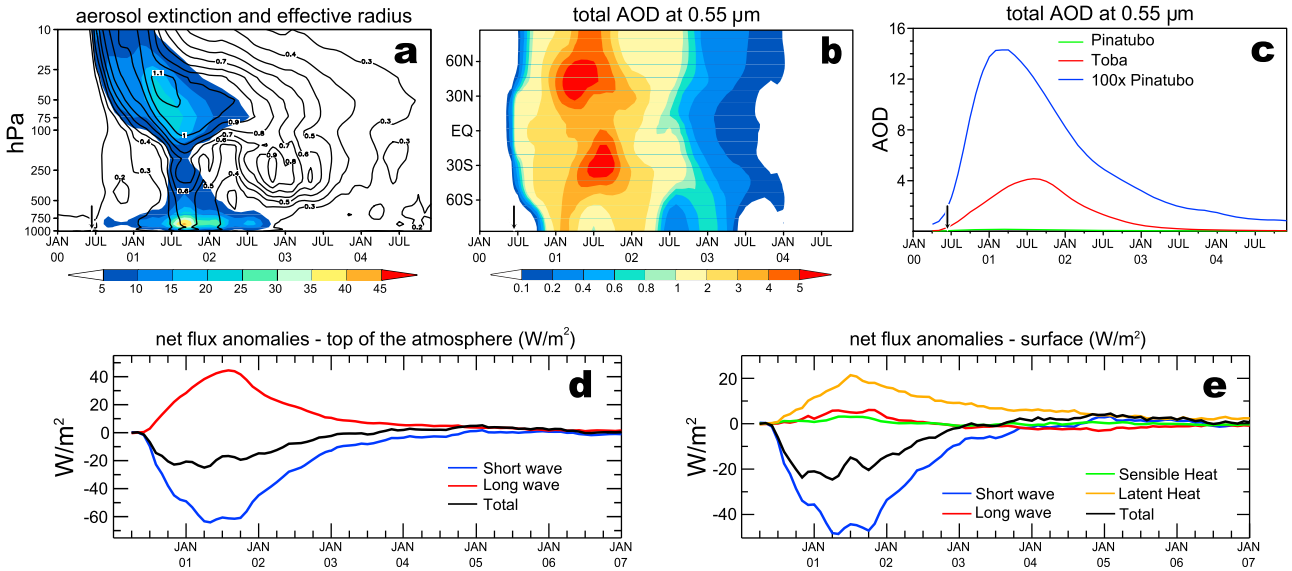

Figure 1. (top) Volcanic aerosol parameters simulated by the aerosol climate model and used as forcing for the ESM. (a) Evolution of aerosol extinction (10^5 m^{-1}) (shading) in the different model layers and effective radius (contour lines) in μm zonally averaged between 10°N and 10°S. The eruption is initialized in June year 00 (black arrow). (b) Hovmoeller diagram of zonally and vertically integrated aerosol optical depth (AOD) at 0.55 μm. (c) 5 month running average of globally and vertically averaged AOD and satellite observations after the Pinatubo eruption [*Sato et al.*, 1993]. (bottom) Monthly averaged global mean flux anomalies for the ensemble mean (W/m^2) with respect to the 2000 year long control run (d) at the top of the atmosphere and (e) at the surface.

[6] In a second step AOD and R_{eff} are used as monthly mean forcing in Max-Planck Institute (MPI) ESM ensemble simulations. The MPI ESM [*Jungclaus et al.*, 2010] with a full carbon cycle implementation consists of the general circulation models for the atmosphere ECHAM5 [*Roeckner et al.*, 2006], and the ocean MPIOM [*Marsland et al.*, 2003] including submodels for land processes, vegetation, and ocean biogeochemistry. ECHAM5 is run at T31 resolution (3.75) with 19 vertical levels, and a model top at 10 hPa. MPIOM applies a conformal mapping grid with a horizontal resolution ranging from 22 km to 350 km. An ensemble of five simulations was performed for the YYT eruption with different initial conditions taken from a 2000 year control run under 800 AD conditions (Figure S1, see auxiliary material for details of experimental set up and both models).[1]

3. Results and Discussions

[7] Immediately after the eruption, initialized in mid June of the first model year (indicated as year 00), SO_2 is oxidized into condensable H_2SO_4 vapor. SO_2 oxidation is delayed when compared with the evolution after the much weaker 1991 Pinatubo eruption due to the limiting factor of OH- abundance [*Bekki*, 1995; *Bekki et al.*, 1996]. Condensational growth and coagulation lead to a maximum AOD (5) and R_{eff} (1.1 μm) about one year after the eruption (summer 01) (Figure 1). Rapid sedimentation of large aerosol particles occurs after the maximum size is reached, so AOD is already at background levels by year four. The aerosol lifetime is therefore smaller than given by *Bekki et al.* [1996] who simulate a lifetime of ten years but with 3.5 times higher sulfur emission. This leads to a slow SO_2 oxidation rate over four years and consequently different particle sizes. *Robock et al.* [2009] with a Pinatubo particle size distribution yield lifetimes of sulfate aerosol in the range of 4 to 8 years comparable with a GISP ice core six year sulfate signal 71 ± 5 ka B.P., which *Zielinski et al.* [1996] attributed to Toba. However, no YTT tephra was found in that layer and no corresponding sulfur signal in any Antarctic ice core could be detected, as would be the case if a tropical eruption had been the source. It may well be the case that the Greenland ice core indicates, e.g., a continued fissure eruption in Iceland. Hence, the duration of the YTT volcanic cloud remains uncertain and the ice core evidence of sulfur emission from the tropical Toba eruption may not hold. R_{eff} persists larger than 1 μm in the densest part of the aerosol layer, indicating much reduced reflectance of solar radiation when compared with a reference Pinatubo (R_{eff} = 0.5 μm) and a background aerosol (R_{eff} = 0.2 μm). Compared to the 100-times Pinatubo AOD [*Sato et al.*, 1993] as used by *Jones et al.* [2005] the AOD maximum occurs six months later, it is a factor of 3.5 smaller, and its e-folding time is reduced by a factor of two to 6.8 months (Figure 1c).

[8] As a result of aerosol coagulation/size/sedimentation effects, the Earth's surface is strongly influenced for only a few years. The maximum monthly averaged global mean flux anomaly for the ensemble mean at the top of the atmosphere (Figure 1d) (Short Wave (SW) −63 W/m^2, Long Wave (LW) +45 W/m^2, and total −18 W/m^2) is still large but much smaller than that in previous simulations: SW −135 W/m^2, LW +75 W/m^2, and total −60 W/m^2 by *Jones et al.* [2005], and SW −100 W/m^2 by *Robock et al.* [2009]. Hence, our more comprehensive simulations lead to strongly reduced radiative flux anomalies compared to earlier results. At the surface (Figure 1e) the massive reduction of incom-

[1]Auxiliary materials are available in the HTML. doi:10.1029/2010GL045464.

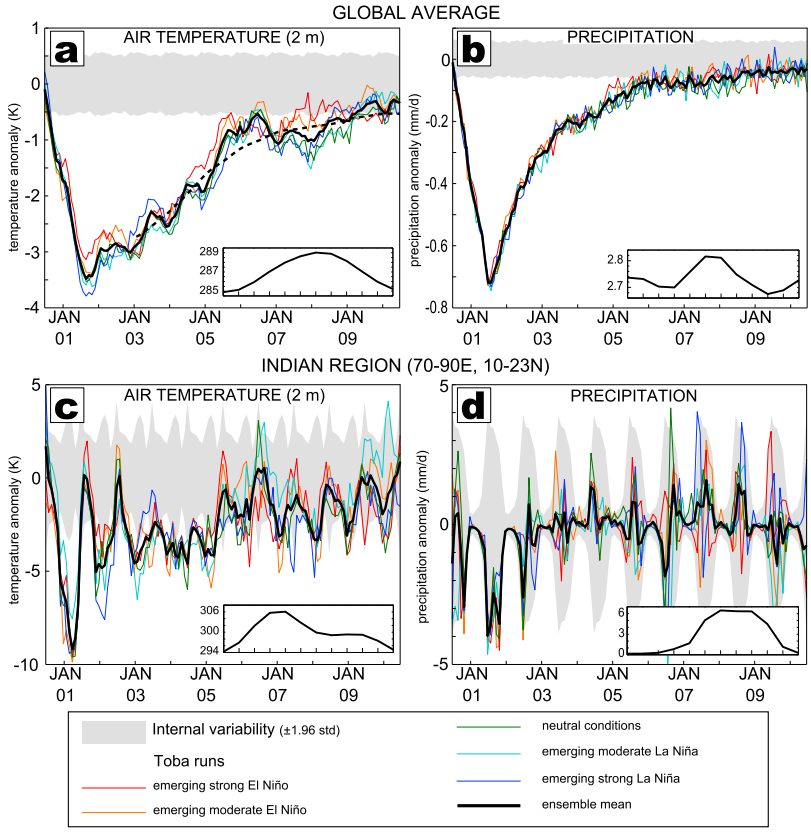

Figure 2. (a, c) Mean temperature and (b, d) precipitation anomalies for the globe (Figures 2a and 2b) and the Indian region (Figures 2c and 2d) for the ensemble mean and individual simulations. The shaded areas denote ±1.96 standard deviations of the control run. The inserts are sketches of the respective climatological annual cycles of the control run. The dashed line in Figure 2a depicts a 3-year running average.

ing shortwave radiation (maximum −49 W/m^2) is in part compensated by increased longwave downwelling radiation from the aerosol, reduced evaporation, and increased sensible heat flux due to fewer clouds. After four years the negative flux anomaly at the surface vanishes and is followed by a slightly positive one due to reduced evaporation from the cooler ocean surface.

[9] Negative global mean surface temperature and precipitation anomalies (Figures 2a and 2b) exceed natural variability for the first nine years after the eruption. While the spread of the precipitation anomalies is small the different initial conditions imply a large spread of the temperature signal. The cold ocean surface temperatures tend to prolong the weak negative global mean temperature anomalies to year ten, i.e., beyond the immediate radiative impact. Maximum global mean cooling for all five simulations is −3.5 K, varying between −3.8 K for anticipated strong La Niña and −3.1 K for anticipated strong El Niño.

[10] In all ensemble members maximum cooling is much smaller and of considerably shorter duration than reported in former model studies. First estimates [*Rampino and Self*, 1992] obtained a similar temperature drop of −3.5 K and in contrast hypothesized a long lasting millennial-scale cooling response. This was based on 1000 Mt of stratospheric aerosol, corresponding to 326 Mt S (38% of our sulfur emission). Coupled atmosphere ocean model studies [*Jones et al.*, 2005; *Robock et al.*, 2009] obtained around −10 K maximum global mean cooling and the return of the signals back to (near) normal variability well beyond a decade for a stratospheric sulfur input comparable to 100Xtimes Pinatubo and a Pinatubo aerosol size distribution.

[11] Since the current discussion whether Toba led to the near-extinction of modern humans 74,000 BP focuses on the conditions on the Indian subcontinent [*Williams et al.*, 2009 and their associated comments: *Balter*, 2010; *Haslam et al.*, 2010], we specifically analyse temperature and precipitation anomalies there (Figures 2c and 2d). Variability of precipitation is small during the winter dry season but very large for the summer monsoon season. Temperature decreases during the first eight years after the eruption, but natural variability is exceeded only in the first five winters for all ensemble members. The first winter stands out with a maximum anomaly of −9.5 K. Already during the second winter the temperature anomaly is reduced to −5 K and then slowly declines in the following years. Summer temperature anomalies remain within the range of natural variability for the first two years after the eruption. Precipitation anomalies are significantly negative over India only during the first two summer monsoon seasons. In both seasons reduced clouds and precipitation counteract the negative radiative flux anomalies since they lead to reduced evaporative cooling and to less reflection of solar radiation due to reduced cloudiness. Once the precipitation anomalies are no longer distinguishable from natural variability in year three, radiative cooling due to volcanic

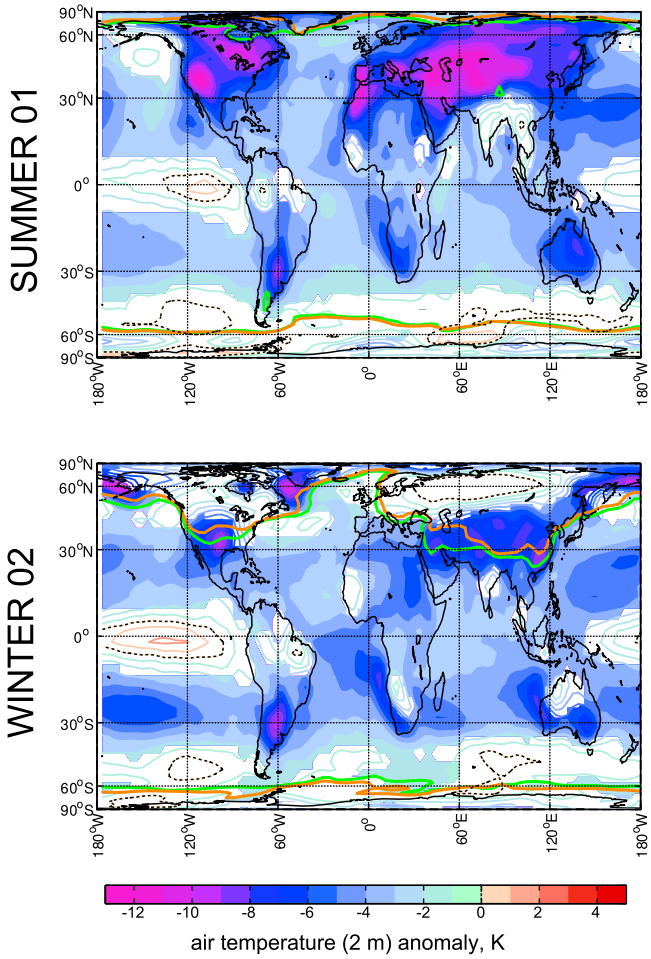

Figure 3. Temperature anomalies (K) for the Northern Hemisphere 1st summer and 2nd winter after the eruption for the ensemble mean. The frost line is included (orange for the control climate and green for the simulations). Line (filled) contours individuate regions where the anomaly is within (exceeds) the thresholds of natural variability, defined as the ±1.96 standard deviations evaluated for the control run. Contours are drawn at 1 K intervals.

aerosol dominates, leading to the cooler summer conditions from year three onwards.

[12] Global temperature anomaly patterns show large spread among the ensemble members introduced by the initial state of the tropical Pacific (Figure 3 for the ensemble mean, for the individual ensemble members see Figures S2 and S3). At mid and high latitudes, differences among the individual simulations are much smaller than in the tropics. In winter, the strongest effects are found in boreal areas in the second year. Only a few regions (Southern U.S. and the Argentinean Pampas) experience strong cooling in winter exceeding −10 K. In all cases, there is a tendency towards positive surface air temperature anomalies over the central eastern tropical Pacific. Another common feature is the positive temperature anomaly over northern Eurasia in winter. Advection of mild moist air from the Atlantic overrides the effect of radiative cooling in this region. This has also been observed after most historic volcanic eruptions [i.e., *Robock and Mao*, 1992].

[13] Summer temperature anomalies are strongest one year after the eruption when widespread cooling exceeding −6 K is found over the northern continents with maximum cooling of −12 K. Over the tropical Pacific, the cooling is generally less severe and becomes stronger with anticipated lower Pacific SSTA, i.e., from anticipated strong El Niño to strong La Niña. Some tropical regions (like India,) even experience warming in case of strong El Niño because less precipitation and clouds counteract the volcano induced radiative effects. The relatively small shifts of the frost line suggest no severe change in environmental conditions that could induce dramatic global-scale alterations in the biosphere. Consistent with temperature changes, precipitation changes are mostly confined to the tropical regions (Figure S4).

[14] The simulation of the climatic effects of the Toba eruption indicates that global mean temperature anomalies are three times weaker than previously suggested. These reduced effects mainly arise from a more complete treatment of stratospheric aerosol formation and growth, leading to much weaker radiative forcing due to larger particle sizes and a faster removal rate. Our results demonstrate that considering microphysical processes is essential for studies of this type.

[15] Our results are strongly dependent on the assumed sulfur injection rate of 850 Mt S. New petrological estimates [*Chesner and Luhr*, 2010] obtained atmospheric sulfur loadings for the YTT two orders of magnitude less than previous studies. Not unlikely the sulfur emission of the YTT was lower than our estimate of 100 times Pinatubo resulting in even smaller AOD values and temperature changes. For example, ESM studies of the 1258 eruption [*Timmreck et al.*, 2009] with a global maximum AOD of 0.625 yield a maximum cooling of −0.98 K (global mean).

[16] The global distribution of temperature anomalies is highly dependent on the initial state of the tropical Pacific, which is unknown for the time of the YTT eruption. Furthermore the climate sensitivity 74,000 BP ago might have been different from that in the present simulations. Presumably, different sensitivities for other climate models would also vary their responses. In India the failure of the summer monsoon during the first two years, together with significant volcanic ash deposition and subsequent detrimental effects on vegetation may have produced the greatest environmental stress [*Haslam et al.*, 2010; *Haslam and Petraglia*, 2010]. The implied muted effects for marine biota is also consistent with evidence suggesting perhaps only one species of plankton in the world ocean may have significantly changed its abundance at this time [*McIntyre et al.*, 1972]. Overall, our simulations of the YTT eruption 74,000 BP suggest that the temperature and precipitation anomalies exceeded natural variability but were not large enough to severely affect the species survival of modern humans.

[17] **Acknowledgments.** This work benefits from stimulating discussions within the MPI-M Super Volcano and Millennium projects. The authors are grateful to Slimane Bekki and Sebastian Rast for their help with the OH parameterization. D.Z. acknowledges funding by the ENIGMA project from the Max Planck Society. This publication is contribution 206 of the Sonderforschungsbereich 574 "Volatiles and Fluids in Subduction Zones" at Kiel University. Computations were done at the German Climate Computer Center (DKRZ).

References

Ambrose, S. H. (1998), Late Pleistocene human population bottlenecks, volcanic winter, and differentiation of modern humans, *J. Hum. Evol.*, *34*, 623–651.

Balter, M. (2010), Of two minds about Toba's impact, *Science*, *237*, 1187–1188.

Bekki, S. (1995), Oxidation of volcanic SO_2: A sink for stratospheric OH and H_2O, *Geophys. Res. Lett.*, *22*, 913–916.

Bekki, S., J. A. Pyle, W. Zhong, R. Toumi, J. D. Haigh, and D. M. Pyle (1996), The role of microphysical and chemical processes in prolonging the climate forcing of the Toba Eruption, *Geophys. Res. Lett.*, *23*, 2669–2672.

Chesner, C. A., and J. Luhr (2010), Melt inclusion study of the Toba Tuffs, Sumatra, Indonesia, *J. Volcanol. Geotherm. Res.*, doi:10.1016/j.jvolgeores.2010.06.001, in press.

Chesner, C. A., W. I. Rose, A. Deino, R. Drake, and J. A. Westgate (1991), Eruptive history of Earth's largest Quaternary caldera (Toba, Indonesia) clarified, *Geology*, *19*, 200–203.

Haslam, M., and M. Petraglia (2010), Comment on "Environmental impact of the 73 ka Toba super-eruption in South Asia" by M. A. J. Williams et al., *Palaeoclimatol., Palaeoecol., Palaeogeogr.*, *296*, 199–203.

Haslam, M., et al. (2010), The 74 ka Toba super-eruption and southern Indian hominins: Archaeology, lithic technology and environments at Jwalapuram Locality 3, *J. Archaeol. Sci.*, *37*, 3370–3384, doi:10.1016/j.jas.2010.07.034.

Jones, G. S., J. M. Gregory, P. A. Stott, S. F. B. Tett, and R. B. Thorpe (2005), An AOGCM simulation of the climate response to a volcanic super-eruption, *Clim. Dyn.*, *25*, 725–738.

Jungclaus, J. H., et al. (2010), Climate and carbon-cycle variability over the last millennium, *Clim. Past*, *6*, 723–737.

Louys, J. (2007), Limited effect of the Quaternary's largest super-eruption (Toba) on land mammals from Southeast Asia, *Quat. Sci. Rev.*, *26*, 3108–3117.

Marsland, S. J., et al. (2003), The Max Planck Institute global ocean/sea ice model with orthogonal curvilinear coordinates, *Ocean Modell.*, *5*, 91–127.

McIntyre, A., W. F. Ruddiman, and R. Jantzen (1972), Southward Penetrations of the North Atlantic Polar Front: Faunal and floral evidence of large-scale surface water mass movements over the last 225,000 years, *Deep Sea Res.*, *19*, 61–77.

Niemeier, U., et al. (2009), Initial fate of fine ash and sulfur from large volcanic eruptions, *Atmos. Chem. Phys.*, *9*, 9043–9057.

Oppenheimer, C. (2002), Limited global change due to the largest known Quaternary eruption, Toba 74 kyr BP?, *Quat. Sci. Rev.*, *21*, 1593–1609.

Petraglia, M., et al. (2007), Middle Paleolithic assemblages from the Indian subcontinent before and after the Toba Super-Eruption, *Science*, *317*, 114–116.

Pinto, J. P., R. P. Turco, and O. B. Toon (1989), Self-limiting physical and chemical effects in volcanic eruption clouds, *J. Geophys. Res.*, *94*, 11,165–11,174.

Rampino, M. R., and S. Self (1992), Volcanic winter and accelerated glaciation following the Toba super-eruption, *Nature*, *359*, 50–52.

Robock, A., and J. Mao (1992), Winter warming from large volcanic eruptions, *Geophys. Res. Lett.*, *19*, 2405–2408.

Robock, A., C. M. Ammann, L. Oman, D. Shindell, S. Levis, and G. Stenchikov (2009), Did the Toba volcanic eruption of ~74 ka B.P. produce widespread glaciation?, *J. Geophys. Res.*, *114*, D10107, doi:10.1029/2008JD011652.

Roeckner, E., et al. (2006), Sensitivity of simulated climate to horizontal and vertical resolution in the ECHAM5 atmosphere model, *J. Clim.*, *19*, 3771–3791.

Rose, W. I., and C. A. Chesner (1987), Dispersal of ash in the great Toba eruption, 75 ka, *Geology*, *15*, 913–917.

Sato, M., J. E. Hansen, M. P. McCormick, and J. B. Pollack (1993), Stratospheric aerosol optical depths, 1850–1990, *J. Geophys. Res.*, *98*, 22,987–22,994.

Self, S., and S. Blake (2008), Consequences of explosive supereruptions, *Elements*, *4*, 41–46.

Stier, P., et al. (2005), The aerosol climate model ECHAM5-HAM, *Atmos. Chem. Phys.*, *5*, 1125–1156.

Timmreck, C., S. J. Lorenz, T. J. Crowley, S. Kinne, T. J. Raddatz, M. A. Thomas, and J. H. Jungclaus (2009), Limited temperature response to the very large AD 1258 volcanic eruption, *Geophys. Res. Lett.*, *36*, L21708, doi:10.1029/2009GL040083.

Whiteside, J. H., P. E. Olson, T. M. Eglinton, E. Brookfiled, and R. N. Sambrrotto (2010), Compound-specific carbon isotopes from Earth's largest flood basalt eruptions directly linked to the end-Triassic mass extinction, *Proc. Natl. Acad. Sci. U. S. A.*, *107*, 6721–6725, doi:10.1073/pnas.1001706107.

Wignall, P. B. (2005), The link between large igneous province eruptions and mass extinctions, *Elements*, *1*, 293–297.

Williams, M. A. J., et al. (2009), Environmental impact of the 73 ka Toba super-eruption in South Asia, *Palaeoclimatol., Palaeoecol., Palaeogeogr.*, *284*, 295–314.

Zielinski, G. A., P. A. Mayewski, L. D. Meeker, S. Whitlow, M. S. Twickler, and K. Taylor (1996), Potential atmospheric impact of the Toba Mega-Eruption ~71,000 years ago, *Geophys. Res. Lett.*, *23*, 837–840, doi:10.1029/96GL00706.

T. J. Crowley, School of GeoSciences, University of Edinburgh, West Main Road, Edinburgh EH9 3JY, UK.

H.-F. Graf, Centre Atmospheric Science, University of Cambridge, Lensfield Road, Cambridge CB2 1EW, UK.

J. H. Jungclaus, S. J. Lorenz, D. Matei, U. Niemeier, C. Timmreck, and D. Zanchettin, Max-Planck Institute for Meteorology, Bundesstr. 53, D-20146 Hamburg Germany. (claudia.timmreck@zmaw.de)